A Generalised Spatio-Temporal Registration Framework for Dynamic PET Data: Application to Neuroreceptor Imaging

Jieqing Jiao[1,2,⋆], Julia A. Schnabel[1], and Roger N. Gunn[1,2,3]

[1] Institute of Biomedical Engineering, Department of Engineering Science, University of Oxford, UK
[2] Imanova Limited, Hammersmith Hospital, London, UK
[3] Department of Medicine, Imperial College, London, UK

Abstract. This work presents a novel pharmacokinetic model based registration algorithm for the motion correction of dynamic positron emission tomography (PET) images. The algorithm employs a generalised model that derives the input function from the tomographic data itself to model the PET tracer kinetics and thus eliminates the need of arterial blood sampling. Both the temporal constraint from the tracer kinetic behaviour and spatial constraint from the image similarity are integrated in a joint probabilistic model, in which the subject motion and tracer kinetic parameters are iteratively optimised, leading to a groupwise registration framework of motion corrupted dynamic PET data. The algorithm is evaluated with simulated and measured human dopamine D3 receptor imaging data using [^{11}C]-(+)-PHNO. The simulation-based validation demonstrates that the new algorithm has a subvoxel registration accuracy on average for noisy data with simulated motion artefacts. The algorithm also shows reductions in motion on initial experiments with measured clinical [^{11}C]-(+)-PHNO brain data.

Keywords: Groupwise spatio-temporal registration, dynamic PET, motion correction, basis pursuit denoising.

1 Introduction

Positron emission tomography (PET) is a powerful non-invasive imaging tool that can provide valuable biological measurements of physiology, biochemistry and pharmacology. These measurements readily enable the investigation of normo-patho-physiology and aid in drug development by providing important information on whether a drug reaches and engages with its target. A modern PET scanner has a spatial resolution of $4mm$, and subject motion inevitably alters the voxel-to-tissue mapping during a dynamic scan of between 30 minutes to 2 hours. The corrupted tissue activity curves measured cause inaccuracies

⋆ This work is supported by Chinese Ministry of Education - University of Oxford Scholarships and Clinical Imaging Centre, GlaxoSmithKline.

K. Mori et al. (Eds.): MICCAI 2013, Part I, LNCS 8149, pp. 211–218, 2013.

in quantifying the relevant biological/physiological processes. Thus, motion correction for quantitative dynamic PET is critical. For image-based registration methods, this is technically challenging since the similarities of morphological features or temporally consistent information is more limited in PET frames compared with magnetic resonance imaging (MRI) or computed tomography (CT) [1]. To address such image registration problems in dynamic imaging, kinetic models have been introduced to account for temporal changes in MRI data [2]. For dynamic PET data, we previously presented an approach [3] that incorporates a tracer pharmacokinetic model into the registration framework to correct for subject motion. This data-driven pharmacokinetic model required a blood input function to describe different tracer behaviour across the images. This means that the method is limited to data sets that have associated measurements of the arterial input function, which represent only a small fraction of dynamic PET studies. The goal of this work is to develop a method which generalises to dynamic PET studies that do not have such measurements.

In this paper we develop a novel registration framework for dynamic PET images using a generalised pharmacokinetic model. A reference region is selected in the imaged volume with no (or lowest) specific binding. The input function is derived from the reference region and therefore eliminates the blood-dependence. The unknown compartmental system is solved with a set of kinetic basis functions and basis pursuit denoising. The basis pursuit denoising approach depends on the estimation of a relaxation parameter which determines the parsimony of the kinetic model. We propose an efficient approach for its estimation. To the best of our knowledge, this work presents the first algorithm in literature to correct for subject motion by incorporating a generalised pharmacokinetic model into the registration of dynamic PET data.

2 Method

2.1 Joint Probabilistic Model of Tracer Kinetics and Subject Motion

Whist the process of radioactive decay gives rise to a Poisson distribution, in reconstructed PET image data, the distribution resembles a Gaussian due to the aggregation of a number of noise sources [4]. For each image volume, the tracer kinetics of the injected tracer determines the intensity of photon emission. However, any subject motion will affect the voxel-to-tissue mapping. Therefore, given the measured PET data $\mathbf{Y}$, the probability of tracer kinetics $\mathbf{\Phi}$ and subject motion $\mathbf{T}$ can be formulated as:

$$p(\mathbf{\Phi}, \mathbf{T}|\mathbf{Y}) = \prod_{j=1}^{M} \prod_{k=1}^{F} \frac{1}{\sqrt{2\pi\sigma^2(t_k)}} exp\left(-\frac{(\mathbf{Y}(\mathbf{T}_k^{-1}(\mathbf{x}_j), t_k) - \mathbf{Y}_{\mathbf{\Phi}}(\mathbf{x}_j, t_k))^2}{2\sigma^2(t_k)}\right), \tag{1}$$

where $Y_{\mathbf{\Phi}}$ is the tracer activity in the image volume determined by $\mathbf{\Phi}$, $\mathbf{x}_j$ are the coordinates of voxel j, t_k is the mid-frame time for the $k-$th frame, and M and F are the numbers of voxels and time frames, respectively. $\sigma^2(t_k) = c \times \mathbf{Y}(t_k)$ is the noise variance where c is a noise level constant.

2.2 Basis Pursuit Reference Tissue Model

The tracer activity, $\mathbf{Y_\Phi}$, can be described by a generalised reference tissue model [5]. Let $C_T(t)$ and $C_R(t)$ be tracer concentration time courses in a target and reference tissue, respectively. Then, the general equation for a reference tissue input compartmental model is $C_T(t) = \phi_0 C_R(t) + \sum_{i=1}^{m+n-1} \phi_i e^{-\theta_i t} \otimes C_R(t)$, where m and n are the total numbers of tissue compartments in the target and reference tissues, and $\otimes$ denotes convolution [5].

This can be expressed as an expansion on a basis, $C_T(t) = \sum_{i=1}^{N} \phi_i \psi_\mathbf{i} = \mathbf{\Phi\Psi}$, with $\psi_\mathbf{i} = e^{-\theta_i t} \otimes C_R(t)$. A discrete set of $N = m + n - 1$ values for θ_i can be chosen from a physiologically plausible range spaced in a logarithmic manner to elicit a suitable coverage of the kinetic spectrum.

The tissue observation $\mathbf{y} = Y(x_j)$, corresponds to $C_T(t)$ as $\mathbf{y} = [y_1 \cdots y_F]^T$, $y_k = \frac{1}{t_k^e - t_k^s} \int_{t_k^s}^{t_k^e} C_T dt$, where t_k^s and t_k^e are the start and end frame times ($k = 1 \ldots F$). Accordingly, the basis function ψ_i can be written as $\psi_i = [\psi_{i1} \ldots \psi_{iF}]^T$, $\psi_{ik} = \frac{1}{t_k^e - t_k^s} \int_{t_k^s}^{t_k^e} e^{-\theta_i t} \otimes C_R dt$ and $\Psi = [\psi_1 \ldots \psi_N]$. Using the measured PET data $\mathbf{Y}$ and pre-calculated Ψ, the unknown $\mathbf{\Phi}$ can be determined by $\mathbf{Y} \cong \Psi\mathbf{\Phi}$. To account for the temporally varying statistical uncertainty of the measurements, the weighted least squares problem $\mathbf{W}^{\frac{1}{2}}\mathbf{Y} \cong \mathbf{W}^{\frac{1}{2}}\Psi\mathbf{\Phi}$ can be considered, where $\mathbf{W}$ is the inverse of the covariance matrix.

To solve for $\mathbf{\Phi}$, standard least squares techniques are not usually applicable because an overcomplete basis ($N > F - 1$) leads to an under-determined set of equations. In [5], the problem is transformed by applying the method of basis pursuit denoising [6] by introducing a regularising term on sparsity, to $\min_\mathbf{\Phi} ||\mathbf{W}^{\frac{1}{2}}(\mathbf{Y} - \Psi\mathbf{\Phi})||_2^2 + \mu||\mathbf{\Phi}||_p$. The regularisation parameter $\mu > 0$ balances the approximation error and sparseness of $\mathbf{\Phi}$ to impose a unique solution. This is based on prior knowledge that the observed data can be accurately described by a few compartments. For computational purposes, this corresponds to $p = 1$ being chosen for the L_p norm and the problem is solved by basis pursuit denoising as $\min \frac{1}{2}\mathbf{x}^T\mathbf{H}\mathbf{x} + \mathbf{c}^T\mathbf{x} \quad s.t. \quad x_i \geq 0$ where $\mathbf{H} = \begin{bmatrix} \Psi^T\mathbf{W}\Psi & -\Psi^T\mathbf{W}\Psi \\ -\Psi^T\mathbf{W}\Psi & \Psi^T\mathbf{W}\Psi \end{bmatrix}$, $\mathbf{c} = \mu\mathbf{1} - \begin{bmatrix} \Psi^T\mathbf{W}\Psi \\ -\Psi^T\mathbf{W}\Psi \end{bmatrix}$ and $\mathbf{x} = \begin{bmatrix} \mathbf{\Phi}^+ \\ \mathbf{\Phi}^- \end{bmatrix}$. $\mathbf{\Phi}$ is given by $\mathbf{\Phi} = \mathbf{\Phi}^+ - \mathbf{\Phi}^-$ finally yielding $\mathbf{Y_\Phi} = \Psi\mathbf{\Phi}$.

2.3 Determination of Regularisation Parameter μ

μ regularises the number of compartmental components and should be determined by the tracer-target interaction. In [5], μ is selected by leave-one-out cross-validation (LOOCV) using measured $\mathbf{Y}$. For the motion correction task, if determined by LOOCV using data with motion artefacts, μ can be too small, which leads to overfitting of unwanted motion artefacts. Therefore, we optimise μ using a different approach:

Firstly a numerical phantom is needed for the given tracer to provide reconstructed noiseless motion-free 4D PET data $\mathbf{Y}_0$ as the ground truth. In the

volume, we can sample $\mathbf{y}_0$ from $\mathbf{Y}_0$ for each voxel, and add Gaussian noise at a random level to simulate the measured $\mathbf{y}$. Then a set $\mathbb{T} = \{z_1 \dots z_n\}, z_i = (\mathbf{y}, \mathbf{y}_0)$ can be obtained. For $\mathbf{y}$, the basis pursuit denoising regularised by μ can predict a fitted $f_\mu(\mathbf{y})$. For $\mathbb{T}$, the average squared error of f_μ is $L_\mu = \mathbb{E}(f_\mu(\mathbf{Y}) - \mathbf{Y}_0)$. Then we choose the μ that minimises L.

2.4 Iterative Optimisation of Φ and T: A Spatio-Temporal Registration

The joint probability distribution $p(\mathbf{\Phi}, \mathbf{T}|\mathbf{Y})$ is optimised with the Iterated Conditional Modes (ICM) optimisation algorithm [7], consisting of iterating the optimisation of two subsets of the unknowns: $\mathbf{\Phi}$ and $\mathbf{T}$. The iterative optimisations of $p(\mathbf{\Phi}|\mathbf{T}, \mathbf{Y})$ and $p(\mathbf{T}|\mathbf{\Phi}, \mathbf{Y})$ are equivalent to performing basis pursuit denoising to update $\mathbf{\Phi}$, and a spatial similarity minimisation to update $\mathbf{T}$.

Algorithm. Spatio-temporal pharmacokinetic model based registration of 4D PET data

Input: Motion-corrupted PET data $\mathbf{Y}(\mathbf{x}, t)$
Output: Motion-corrected PET data $\mathbf{Y}(\mathbf{T^{-1}}(\mathbf{x}), t)$. The estimated motion $\mathbf{T}$ and tracer pharmacokinetic parameter $\mathbf{\Phi}$.
Initialization $\mathbf{T} = \mathbf{Id}$, $\mathbf{Y}(\mathbf{T^{-1}}(\mathbf{x}), t) = \mathbf{Y}(\mathbf{x}, t)$;
while *not converged* **do**
- Derive reference input $C_R(t)$ from $\mathbf{Y}(\mathbf{T^{-1}}(\mathbf{x}), t)$ and calculate basis function Ψ as in Sec 2.2;
- Do basis pursuit denoising using $\mathbf{Y}(\mathbf{T^{-1}}(\mathbf{x}), t)$ and Ψ, calculating the kinetic parameter $\mathbf{\Phi}$ and the model-predicted PET data $\mathbf{Y_\Phi} = \Psi\mathbf{\Phi}$ as in Sec 2.2;
- Selectively scale $\mathbf{Y}$ and $\mathbf{Y_\Phi}$ using the noise variance term σ as in Sec 2.1, ruling out the voxels containing mainly noise;
- Do image registration on scaled $\mathbf{Y}$ and $\mathbf{Y_\Phi}$ using SSD as the cost function to obtain motion $\mathbf{T}$ and the motion-corrected PET data $\mathbf{Y}(\mathbf{T^{-1}}(\mathbf{x}), t)$;
end

3 Experiments and Results

We applied the proposed method on data from human dopamine D3 receptor imaging studies with [^{11}C]-(+)-PHNO. Dopamine D3 receptors are involved in the pathophysiology of a number of neuropsychiatric conditions such as addiction, schizophrenia, and Parkinson's disease (PD). [^{11}C]-(+)-PHNO is a D3 preferring PET tracer which has recently opened the possibility of imaging D3 receptors in the human brain *in vivo* [8] in various brain structures, such as the substantia nigra (SN), globus pallidus (GP), ventral striatum (VST), dorsal putamen (PU), dorsal caudate (CD) and thalamus (THA). The cerebellum is used as the reference region as it has a low level of specific binding and has been determined to be an appropriate reference tissue for [^{11}C]-(+)-PHNO previously [8].

We used a software phantom to determine the regularisation parameter μ and quantify the motion correction accuracy. The Zubal brain phantom is widely applied in simulating PET neurological images [1,9] but lacks the delineation of SN and VST, which are ROIs in this study. We thus derived the motion free phantom by fitting the tracer kinetic model to measured [^{11}C]-(+)-PHNO 4D data from a healthy subject with visually negligible motion. The PET image voxel size is $2 \times 2 \times 2mm^3$ and the phantom comprises 26 temporal frames (durations: 8×15 s, 3×1 min, 5×2 min, 5×5 min, 5×10 min). Accuracy of registration was quantified as the target registration error (TRE) [10], averaged over all voxels and time frames.

3.1 Regularisation Parameter μ

A set $\mathbb{T}$, $n(\mathbb{T}) = 3000$, was generated using the phantom described above. A mask was applied to discard background voxels with noise only. 50 values for μ were logarithmically spaced in $[10^{-2}, 10^{2}]$. The average squared error L_μ was calculated and is shown in Fig. 1. It is consistent with a histogram of μ that minimises the fitting error for each data point in $\mathbb{T}$. A value of $\mu = 8.6850$ was chosen to be optimal.

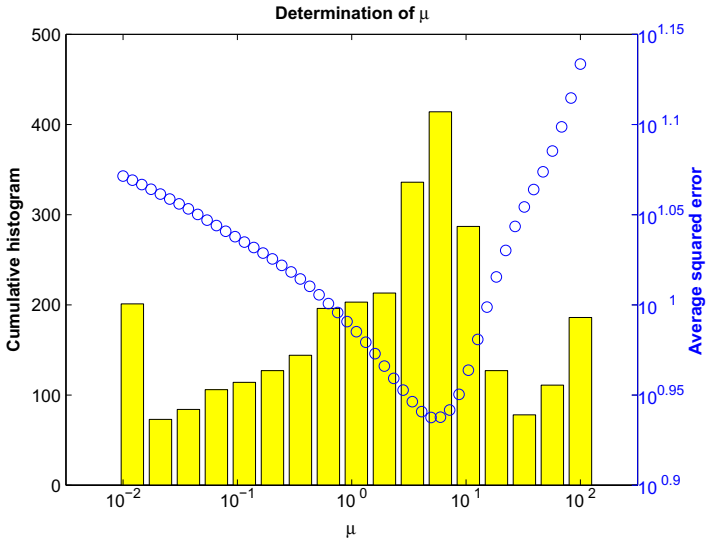

Fig. 1. Determination of regularisation parameter μ for compartmental sparsity for basis pursuit denoising in the registration framework. For 50 μ values logarithmically spaced in $[10^{-2}, 10^{2}]$, the average squared error L_μ (in blue) is consistent with the histogram of μ minimising the fitting error for each data point in $\mathbb{T}$ (in yellow) for an optimal value of $\mu = 8.6850$.

An intuitive way of determining μ is to update its value using $\mathbf{Y}(\mathbf{T}^{-1}(\mathbf{x}), t)$ by LOOCV in each iteration. We compared the TRE of updating μ to that of the fixed $\mu = 8.6850$, and the results show that the fixed μ has similar registration

accuracy and is computationally more efficient. Therefore, we used the fixed μ approach for the following experiments.

3.2 Simulation-Based Validation

Simulated data sets were generated by introducing random rigid head translations and rotations to each temporal frame of the phantom. Ten simulations were conducted for a large motion level ($\sim 10mm$) and a small motion level ($\sim 5mm$) respectively, noise was added at a normal level in clinical data and a higher level. 5 simulations were carried out at each noise level to each motion-corrupted data set, generating 220 data sets. We performed motion correction using three methods: a frame-by-frame registration of each PET frame to the one with highest uptake based on normalised mutual information (FBF), the groupwise registration of all frames with spectral analysis that requires the blood input (GIR_SA) *red* previously proposed by us in [3], and the reference tissue groupwise registration of all frames using basis pursuit (GIR_BP) that avoids blood measurement proposed in this paper. The TREs are shown in Fig. 2.

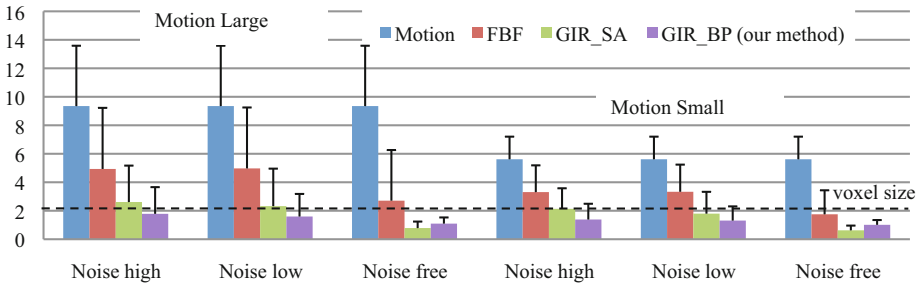

Fig. 2. Registration accuracy, quantified as target registration error (TRE, in mm) of the spatio-temporal groupwise image registration with basis pursuit (proposed GIR_BP), with spectral analysis (GIR_SA, required blood input) and frame-by-frame registration based on normalised mutual information (FBF) on simulated data sets. The dashed line indicates the voxel size. For each simulation, the TREs were averaged over all time frames. The mean TREs at each motion level and noise level before and after correction are shown, along with the standard deviations as error bars. The proposed GIR_BP achieves on average subvoxel ($< 2mm$) accuracy and has smaller errors for noisy data compared to GIR_SA, which requires arterial blood sampling.

3.3 Clinical Data

We applied the GIR_BP method to measured clinical data from a healthy subject with visually obvious motion shown in Fig. 3. [^{11}C]-(+)-PHNO was injected as an intravenous bolus over approximately 30 seconds at the start of a 90 minute 3D-mode dynamic PET acquisition using a Siemens Biograph 6 PET-CT with Truepoint gantry. PET data were reconstructed using 2D filtered back projection with corrections for attenuation (based on a low-dose CT acquisition) and scatter. Dynamic data were binned in the same way as phantom data.

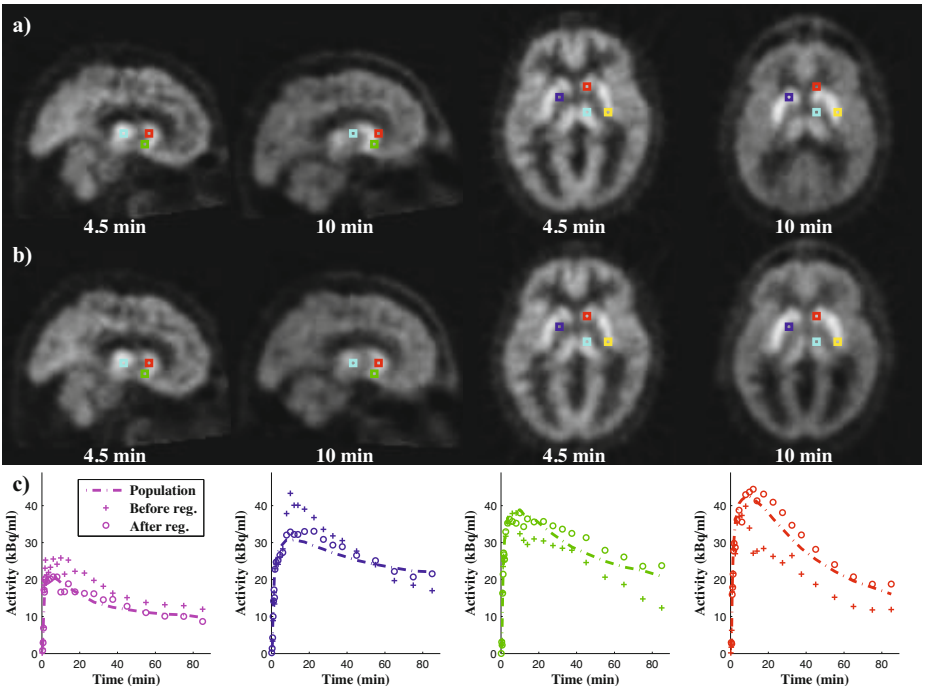

Fig. 3. Selected temporal frames (times are mid-frame times) from sagittal and axial slices from dynamic PET [^{11}C]-(+)-PHNO data of a healthy subject: a) before motion correction, b) after registration using the proposed GIR_BP method. Voxels from various ROIs are depicted in colours which are spatially fixed to demonstrate the displacement. c) PET data from these voxels before and after registration. Mean population PET data (from a larger group of healthy subjects scanned with [^{11}C]-(+)-PHNO) for the ROIs scaled to this subject to account for differences in dose and subject weight is shown by dashed lines. Colours correspond to ROIs as: SN, VST, CD, PU, GP and TH. The subject exhibited obvious rotation of $\sim 10^{\circ}$ which was corrected considerably by the proposed method, and the tracer kinetics in these ROIs determined by the target densities showed consistency with population data after correction.

4 Discussion and Conclusion

We have introduced a generic registration framework to correct for subject motion in dynamic PET data that incorporates a reference tissue pharmacokinetic model into the groupwise registration process. This represents a significant increase in scope over the previous groupwise PET registration method [3] which required arterial blood data and as a consequence would only be applicable to a small number of dynamic PET studies. The new approach incorporates a generic reference tissue model which is implemented in a basis function framework and solved by the method of basis pursuit denoising. We have proposed an efficient approach to determine the relaxation factor that regularises the sparsity of kinetic components in the registration framework. We tested the proposed

method on human dopamine D3 receptor PET data with [^{11}C]-(+)-PHNO with the cerebellum as the reference region. Results on realistic simulated data show subvoxel ($< 2mm$) registration accuracy. Initial evaluation on clinical data from a healthy subject with obvious motion provides evidence that motion can be reduced substantially in line with expectations from the simulated data. The proposed method is in principle applicable to all dynamic PET studies data given the selection of an appropriate reference tissue, as the method is based on an adaptive kinetic model derived from the general properties of compartmental tracer kinetics. Future evaluation over a range of different tracers, and extensions to differing applications requiring higher-order transformations and additional constraints will determine the full utility of the method. In addition, by describing the measured PET data using tracer kinetics and subject motion, the proposed registration framework could be integrated into the reconstruction of sinogram or list-mode data.

References

1. Costes, N., Dagher, A., Larcher, K., Evans, A.C., Collins, D.L., Reilhac, A.: Motion correction of multi-frame PET data in neuroreceptor mapping: simulation based validation. Neuroimage 47(4), 1496–1505 (2009)
2. Buonaccorsi, G.A., Roberts, C., Cheung, S., Watson, Y., Davies, K., Jackson, A., Jayson, G.C., Parker, G.J.M.: Tracer kinetic model-driven registration for dynamic contrast enhanced MRI time series. Med. Image Comput. Comput. Assist. Interv. 8(pt. 1), 91–98 (2005)
3. Jiao, J., Searle, G.E., Tziortzi, A.C., Salinas, C.A., Gunn, R.N., Schnabel, J.A.: Spatial-temporal Pharmacokinetic Model Based Registration of 4D Brain PET Data. In: Durrleman, S., Fletcher, T., Gerig, G., Niethammer, M. (eds.) STIA 2012. LNCS, vol. 7570, pp. 100–112. Springer, Heidelberg (2012)
4. Oikonen, V.: Noise model for PET time-radioactivity curves. Turku PET Centre Modelling report TPCMOD0008 (2003)
5. Gunn, R.N., Gunn, S.R., Turkheimer, F.E., Aston, J.A.D., Cunningham, V.J.: Positron emission tomography compartmental models: a basis pursuit strategy for kinetic modeling. J. Cereb. Blood Flow Metab. 22(12), 1425–1439 (2002)
6. Chen, S.S., Donoho, D.L., Michael, S.A.: Atomic decomposition by basis pursuit. SIAM Journal on Scientific Computing 20, 33–61 (1998)
7. Besag, J.: On the statistical analysis of dirty pictures. Journal of the Royal Statistical Society, Series B (Methodological) 48(3), 259–302 (1986)
8. Searle, G.E., Beaver, J.D., Tziortzi, A., Comley, R.A., Bani, M., Ghibellini, G., Merlo-Pich, E., Rabiner, E.A., Laruelle, M., Gunn, R.N.: Mathematical modelling of [(11)C]-(+)-PHNO human competition studies. Neuroimage 68, 119–132 (2013)
9. Zubal, I.G., Harrell, C.R., Smith, E.O., Rattner, Z., Gindi, G., Hoffer, P.B.: Computerized three-dimensional segmented human anatomy. Med. Phys. 21(2), 299–302 (1994)
10. Fitzpatrick, J., West, J., Maurer Jr., C.R.: Predicting error in rigid-body point-based registration. IEEE Trans. Med. Imaging 17(5), 694–702 (1998)